

Wavefront Sensing and Control with the Many Headed Hydra Modal Basis

J. FOWLER ¹ AND R. DENO STELTER ²

¹*University of California, Santa Cruz
1156 High St
Santa Cruz, CA 95064, USA*
²*UC Observatories
University of California, Santa Cruz
1156 High St
Santa Cruz, CA, 95060, USA*

ABSTRACT

The future of space and ground based telescopes is intimately tied to technology and algorithm development surrounding wavefront sensing and control. Only with cutting edge developments and unusual ideas will we be able to build diffraction limited observatories on the ground that contend with earth-atmosphere, as well as space-based observatories that sense and control for optical aberrations and telescope jitter. There exist a variety of mathematical bases for decomposing wavefront images, including the zonal modal basis, Zernike polynomials, and Fourier modes. However, previous bases have neglected the most vital element of astronomical optics: our field is only as good as the people in it. In this paper we propose a new Many Headed Hydra Modal Basis (hydra heads) for wavefront decomposition, using physical representations of the Adaptive Optics community. We find that the first author makes the best wavefront decomposition, on the order of a correct reconstruction within $\sim 1\%$ of the original turbulence image. We discuss engineering implications of the Many Headed Hydra Modal Basis, as applied to deformable mirror technology and within active and adaptive optics control loops. Finally, we explore predictive control avenues, by positing that the first author being the most effective wavefront predicts a successful future for them as a high contrast imaging scientist.

Keywords: Wavefront Sensing and Control — Adaptive Optics — Predictive Control — Fourier Series — Deformable Mirrors

1. INTRODUCTION

Future advances in astrophysics depend on improving performance our our telescopes and instruments, ranging from verifying sub-Earth exoplanets around surprisingly nearby stars (Lund et al. 2018), to identifying floofs at opical wavelengths (Mayorga et al. 2021), to discovering exigent threats in galaxies far, far away (Lund 2017). The performance of these instruments is inextricably entwined with how well we are able to sense and correct for aberrations in our incoming light – be it from earth-atmosphere, errors built into the telescope system, or often both. Given we start with some representation of phase from an incoming wavefront, and hope to correct it, the next step in this sensing and control problem is a choice of basis. A zonal modal basis (Shatikhina et al. 2020) is intuitively simple – breaking down each wavefront sensor subaperture into its own mode and controlling along zones. Whereas, a Zernike modal basis (Stangalini et al. 2010) builds up an intuition of optical aberrations, framing incoming light in terms of coma, astigmatism, trefoil, etc, that maps to optical defects within our system. Finally, a Fourier modal basis (Fauvarque et al. 2016) decomposes light into sine and cosine waves, and has a natural connection to Fourier transforms into frequency space.

We present the Many Headed Hydra Modal Basis (hydra heads), as a basis that encapsulates the true character of adaptive optics, by encoding the likeness of the very scientists who do it a basis sets. With Section 2, we work through the formalism of the hydra heads. In Section 3 we examine the effectiveness of the hydra heads as used to decompose a sample turbulence image. In Section 4, we discuss wavefront control applications of the hydra heads. Finally, in Section 5 we make our final conclusions about why the first author makes an extremely good basis set.

Table 1. Atmospheric turbulence simulation.

Layer	Velocity	Direction	r_0
	m/s	degrees	cm
1	22.7	246	38.9
2	3.28	71	44.7
3	16.6	294	45.5
4	5.89	150	38.8
5	19.8	14	43.6

NOTE—These conditions were used to simulate an atmospheric turbulence profile as a practical test of the hydrae. We used conditions from [Poyneer et al. \(2007\)](#), because the first author happened to have simulated this atmosphere at high resolution recently. Our final images are simulated at a wavelength of 1630 nm over an 8 meter primary telescope mirror.

2. FORMULATION OF THE MANY HEADED HYDRA MODAL BASIS

Given 16 starting candidate heads, we build the modes by:

1. Making the head into a square image.
2. Converting the image from color to black and white.
3. Rescaling the image from 0-1.
4. Appending a negative valued copy of the image.
5. Increasing the spatial frequency (number of heads) and altering the orientation.

We display one sample hydra head in Figure 1, built with the Debes head.

Appendix A demonstrates an example the `hydra-sim` software used to create the hydra heads. Appendix B scans through a few examples of modes for each input head.

3. EFFICACY AMONG THE HYDRA HEADS

Given an input set of 16 heads, we built a Many Headed Hydra Modal Basis for each head, as described in Section 2. With this suite of hydrae, we can then test them practically, by decomposing a sample turbulence image. Using HCIPy ([Por et al. 2018](#)), we simulate a turbulence profile with 5 wind layers, each with their own velocity and r_0 . Table 1 outlines the atmospheric parameters used to simulate this atmosphere.

Given each hydra head mode starts as a square m by m matrix, which could map to a representation of a turbulence profile binned down to a resolution of $m \times m$, we make the Many Headed Hydra Modal Basis set \mathbf{A} , by flattening each mode to be a column of \mathbf{A} . From there, decomposing a turbulence image becomes a linear algebra problem of the form:

$$\mathbf{A}\vec{x} = \vec{b} \quad (1)$$

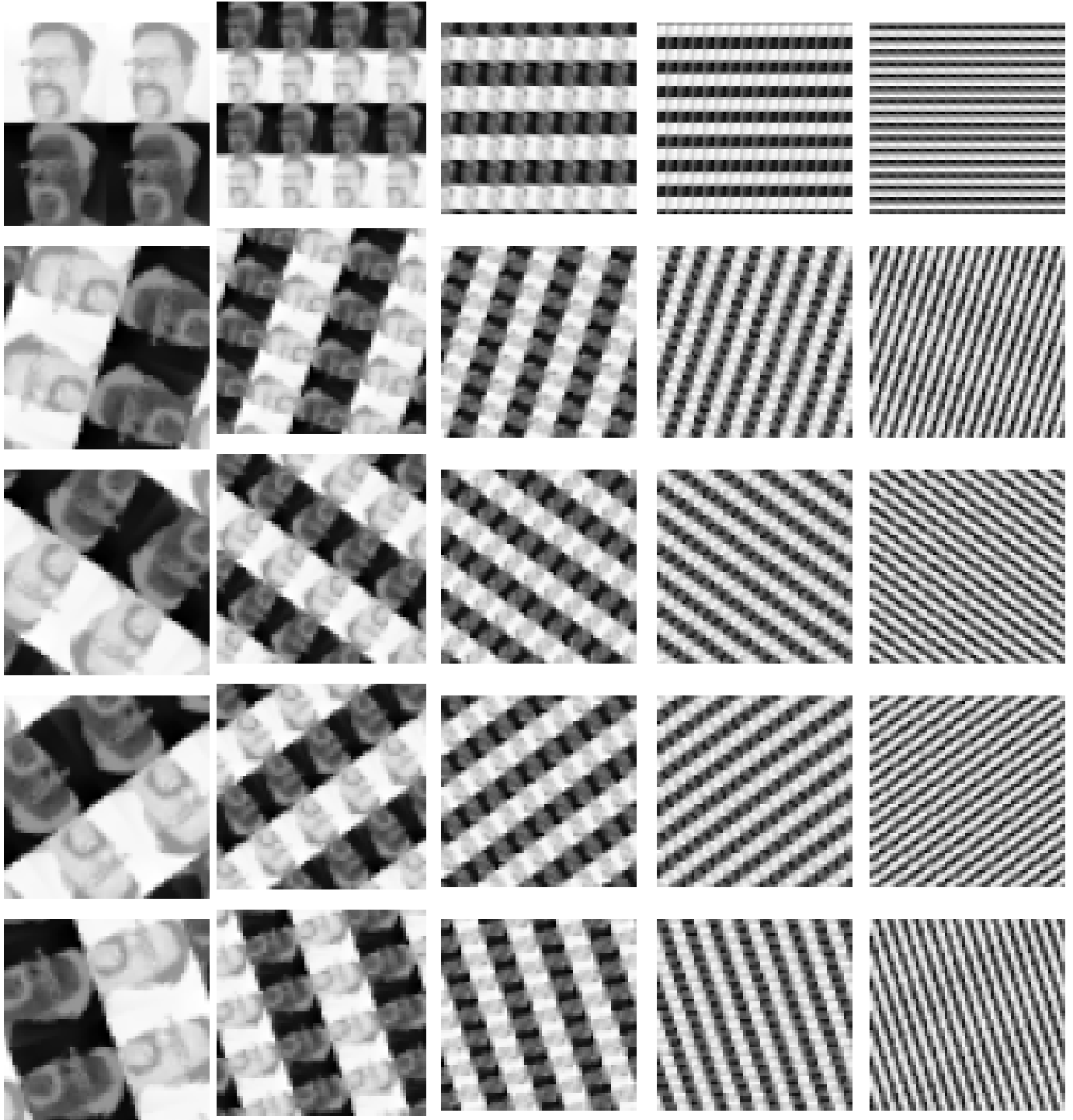


Figure 1. Example Many Headed Hydra Modal Basis set using a Debes head as starting input. While this full set has 2500 modes (spanning tighter degree increments as the pattern rotates and more repetitions of heads) we display a handful of modes to get an idea of the modal basis images.

Table 1. Comparative performance of the hydra heads.

Head	% Error
<i>Hirschauer</i>	0.09
Fowler	1.07
Hinz	1.54
Soumer	2.47
van Belle	2.81
Kirkpatrick	3.81
Macintosh	3.89
Pearce	4.93
Stelter	5.02
Jensen-Clem	5.33
Ngo	5.57
Debes	5.75
Bowens-Rubin	11.97
Steiger	12.34
Lewis	13.92
Balmer	15.66

NOTE—The relative performance of the sample heads. We decompose a sample turbulent wavefront with a hydra head, and calculate the percent difference in the reconstructed image and the original simulated image.

64 where \vec{b} is the flattened image we aim to reconstruct, and \vec{x} contains the coefficients of each mode to reconstruct the
 65 given image. We solve for \vec{x} using a pseudo-inversion of \mathbf{A} , using `numpy`'s singular value decomposition pseudo-inverse
 66 method.

67 For this test we generated 2500 modes for each head, each a 50x50 scene, which was then used to decompose an
 68 image simulated at 100x100 resolution and binned down to match the 50x50 (to preserve Nyquist sampling). Table 1
 69 shows the relative performance of each hydra head. While the Hirschauer head displays the best performance, a closer
 70 inspection of the original input images reveals that the Hirschauer image benefits from a flat background. Considering
 71 the unreliability of dome flats, we rule this out as a potential hydra head, and find that the Fowler hydra head is the
 72 most effective modal basis in this set. Figure 2 shows an example turbulence image and the reconstruction using the
 73 Fowler hydra head. Figure 3 shows the difference image between the reconstruction and the original turbulence.

74 4. CONTROL APPLICATIONS

75 The hydrae are well-suited for pupils produced by off-axis mirrors (such as OAPs or OAEs) because the pupil planes
 76 of off-axis mirrors are tilted with respect to the beam direction resulting in an elongated pupil. The pupil, being
 77 non-square, is thus well-matched to a craftily-cropped head shot, although care must be taken to ensure that the head
 78 shot and the pupil share the same axial length ratio. Deviations can be systematically addressed by adding more
 79 fractal layers, which reduces the problem to one where the solution is known.

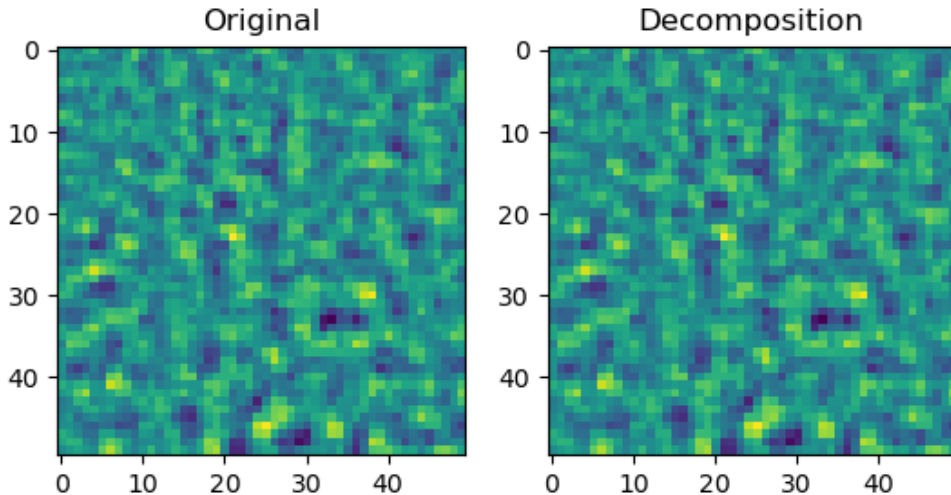


Figure 2. Left: Original scene of turbulence, originally generated at a resolution of 100 pixels under the conditions described in 1, and binned down to 50. Right: Reconstruction using the Fowler hydra head.

80 While head shots of prominent scientists¹ may not, at first, seem to be a sensible basis for wavefront control, we
 81 note that, from the perspective of a deformable mirror (DM) actuator, following a leader is second nature. After all,
 82 a ‘follower/leader’ actuator scheme is a common choice in designing wavefront control loops. We have simplified this
 83 scheme by finding the best head shot and designating it the leader, allowing the DM actuators to act in accordance
 84 with their natural predilections.

85 Edge effect artifacts of the head shots can affect the final result. We have implemented a simple fractal-headed
 86 approach described below, simply allowing the higher frequency features to be fit with (spatially) copies of smaller
 87 head shots as needed.² Determining the lower end cut-off frequency scale when using the hydra heads requires the use
 88 of a carefully-timed application of an integrating sphere fed by a high-powered incandescent lamp or laser, or cryogenic
 89 liquid (we note that open flame light sources are considered more traditional). With some trial and error, the suitable
 90 cut-off frequency can be found experimentally with only mild burns.

91 5. CONCLUSIONS

92 In conclusion, we find that decomposing turbulence with pictures of astronomers is surprisingly feasible, with a
 93 shockingly high variability. While it seemed likely that this project would essentially test how good heads are at
 94 being sin waves, further inspection of the individual bases (see Appendix B) shows a striking similarity at higher order
 95 modes, as only a handful of pixels can be used to represent an image that requires many features to resemble a head.
 96 This potentially implies that the lower order modes are having a large impact on this decomposition.

¹ Or at least the ones who responded to a late-night call on Twitter for head shots.

² We expect that snapshots of stacks of turtles would also be effective.(Green 2019)

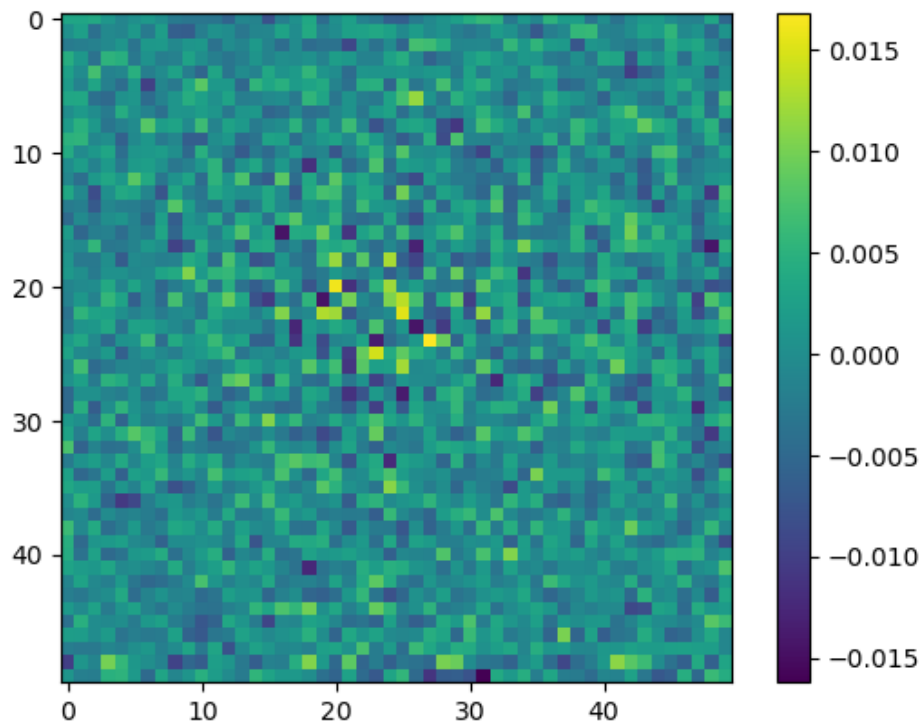


Figure 3. Difference image between the Fowler hydra head reconstruction and the original turbulence. Not the scale on the order of 0.01 radians in the infrared regime.

97 Finally, we stand by the conclusion that how well your head can decompose turbulence is strongly predictive of
 98 scientific output, with a focus on how well the first author can reconstruct the sample scene.³ No formal statistics
 99 have been conducted on this sample to verify this, and we do not recommend this for future works.

100 Thanks to William Balmer, Rachel Bowens-Rubin, John Debes, Alec Hirschauer, Allison Kirkpatrick, Briley Lewis,
 101 Bruce Macintosh, Henry Ngo, Logan Pearce, Phil Hinz, Rebecca Jensen-Clem, Sarah Steiger, Gerard van Belle, and
 102 Remi Soummer for really putting their heads together to make this project possible.

³ This effect has no relation to Fowler sampling (a commonly-used scheme for reading out infrared detectors), as far as we are aware.

103 *Software:* `astropy` (Astropy Collaboration et al. 2018), `matplotlib`, (Hunter 2007), `numpy` (Ferland et al. 2013),
104 `PIL`, (Umesh 2012), `HCIPy`, (Por et al. 2018),

105 APPENDIX

106 A. HYDRAA-SIM SIMULATING THE PERFORMANCE OF THE MANY HEADED HYDRA MODAL BASIS

107 With this paper, we've released `hydra-sim`, allowing any user to generate a modal basis from a square input image,
108 and test it against a turbulence profile. Figure 4 shows an example of using the code to build and test a modal basis.

```
## - IMPORTS
import hydra

|
# Given some data starting square image 400 x 400
image_shape = 400
mode_shape = 32
n_modes = mode_shape**2
head_image = "path/to/your/head_shot.jpg"
hydra.make_modes(head_image, n_modes, modes_out,
                 mode_shape=mode_shape, image_shape=image_shape)

# Given some turbulence data, see how well you basis works
turbulence = "path/to/your/turbulence.fits"
modes = "path/to/your/newly_built_modes.fits"
hydra.test_basis(turbulence, modes)
```

Figure 4. Example code using `hydra-sim` to build a hydra head and decompose an image.

B. FULL SUITE OF HYDRA HEADS

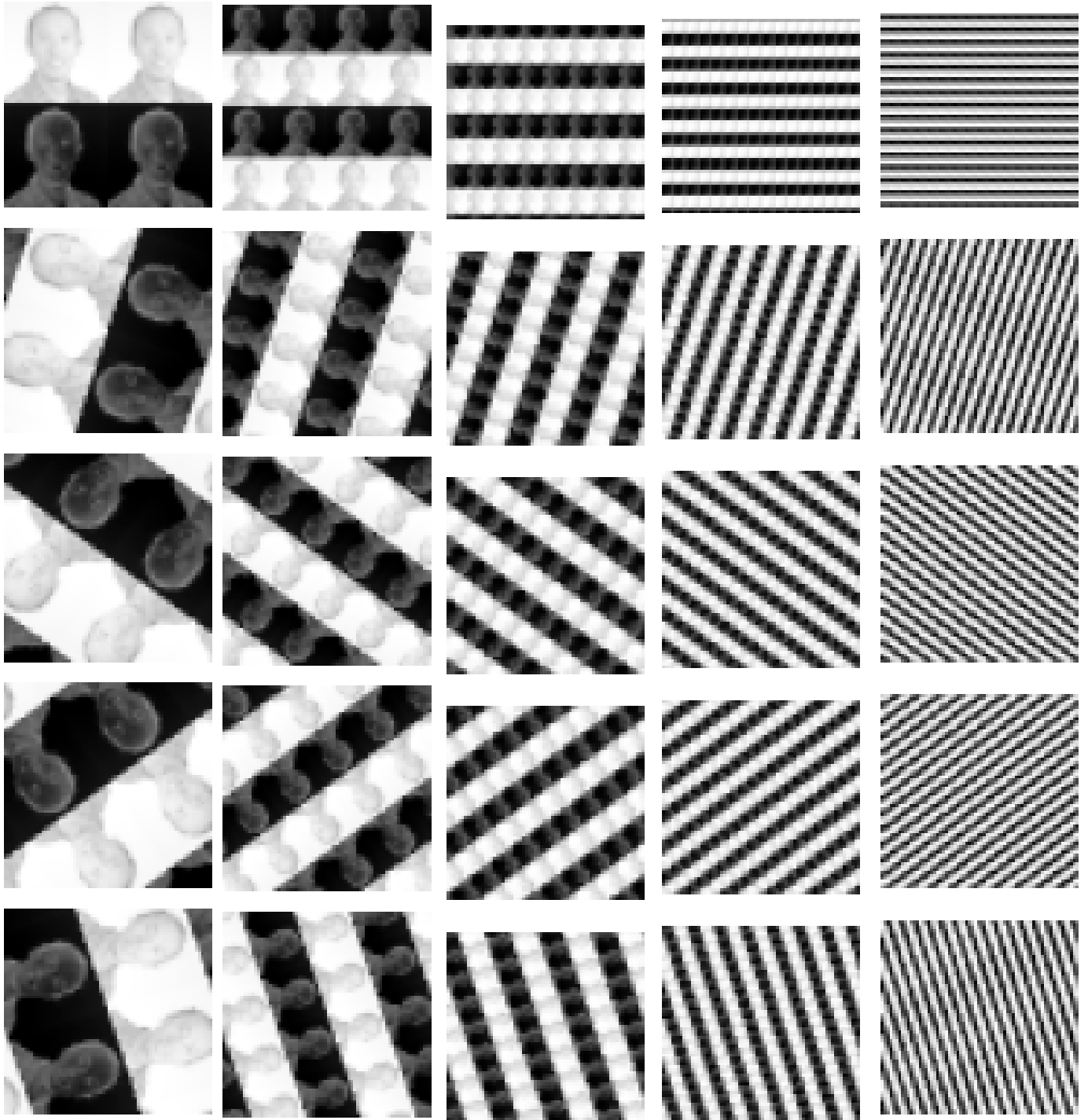
B.1. *Hirschauer Basis*

Figure 5.

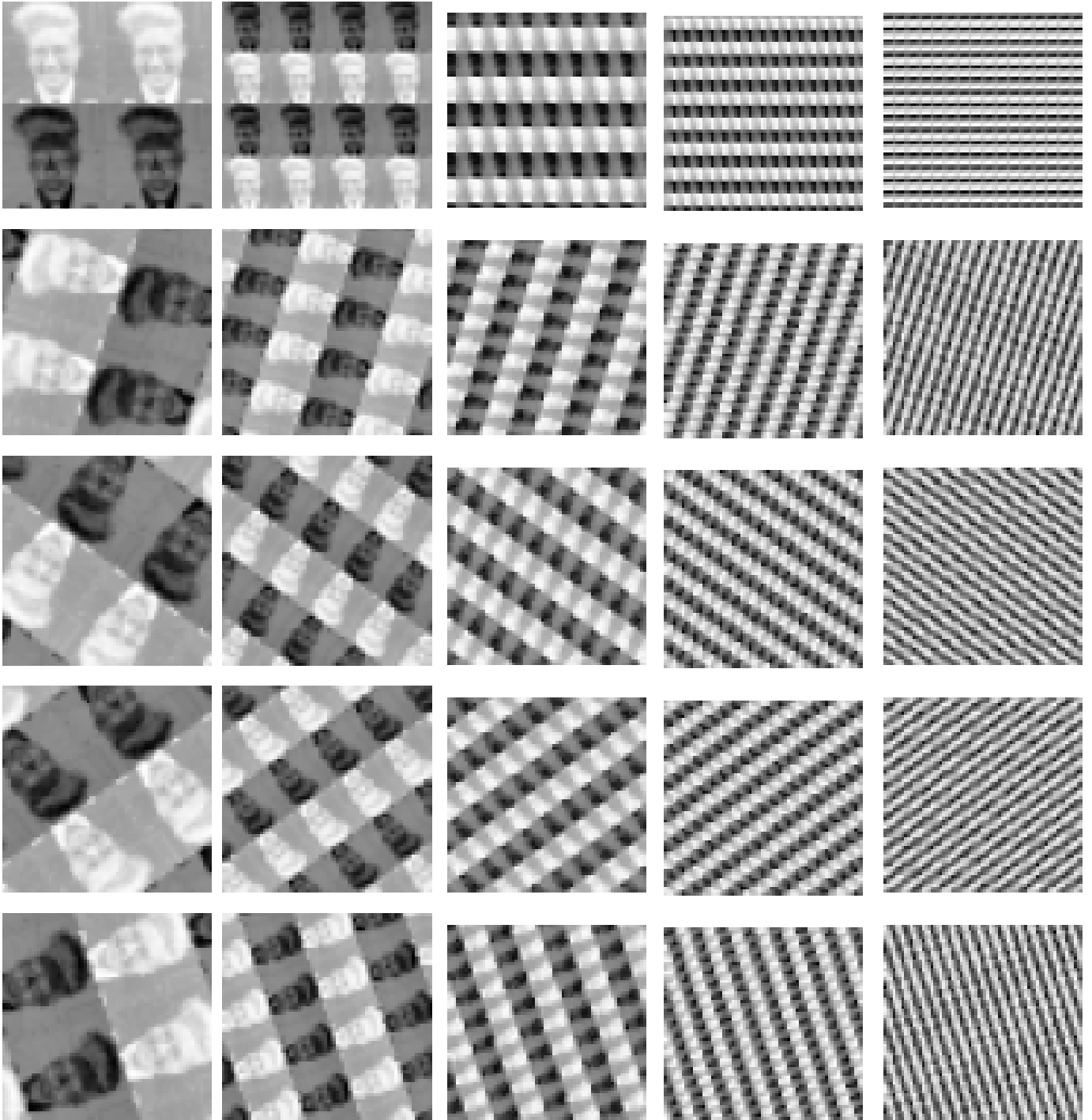
B.2. *Fowler Basis*

Figure 6.

B.3. *Hinz Basis*

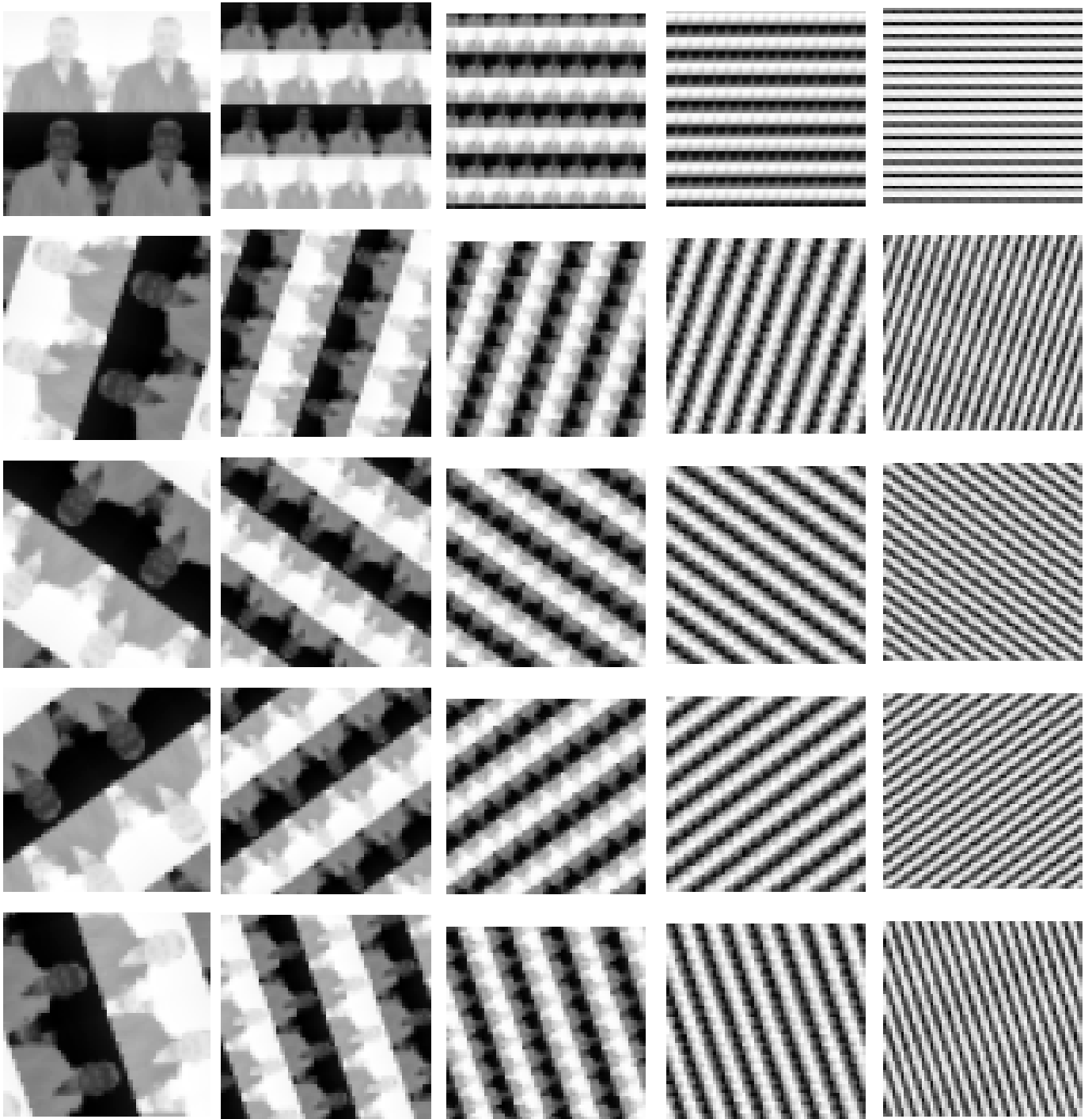


Figure 7.

B.4. *Soummer Basis*

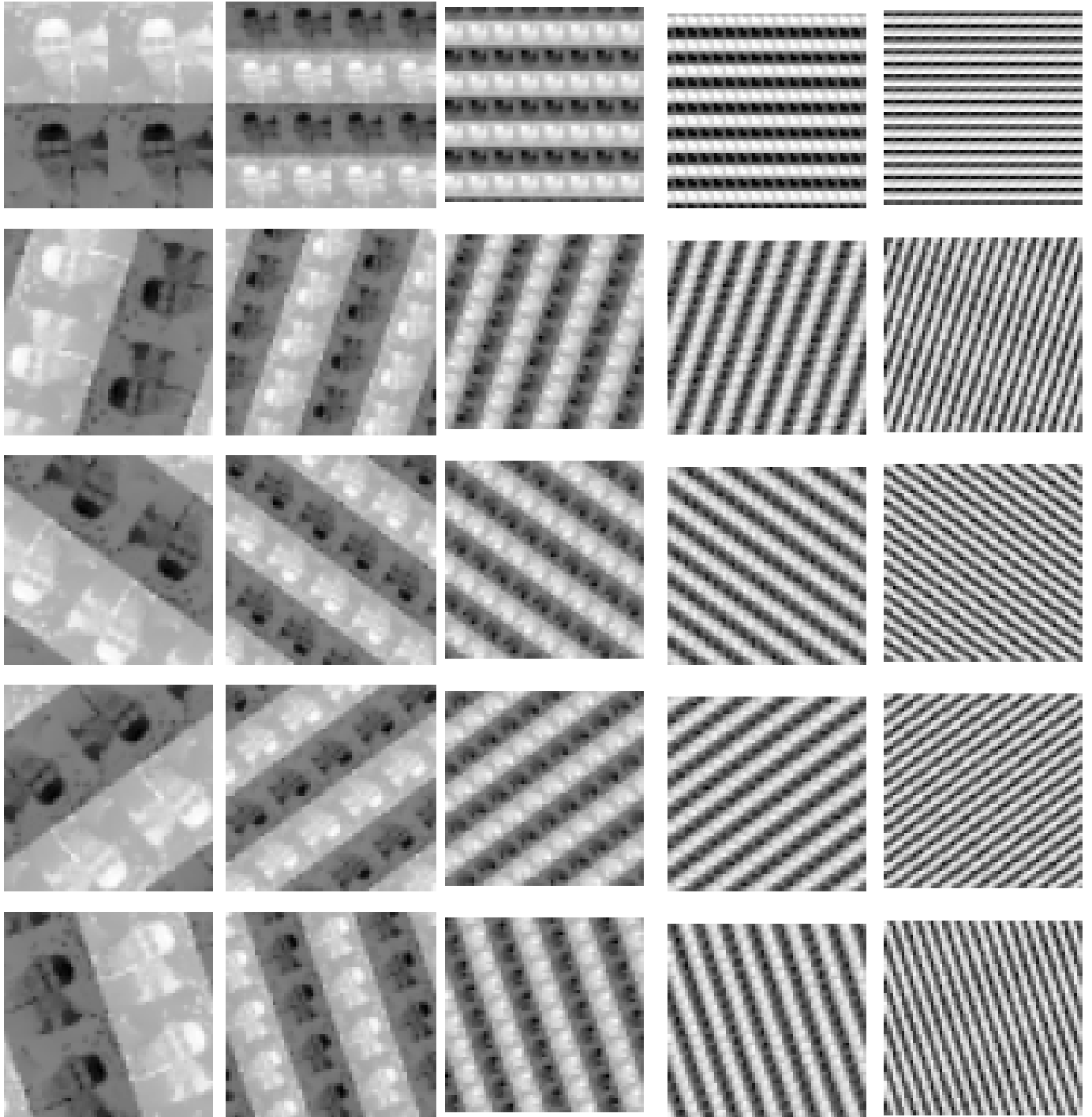


Figure 8.

B.5. *van Belle Basis*

114
116

[b]

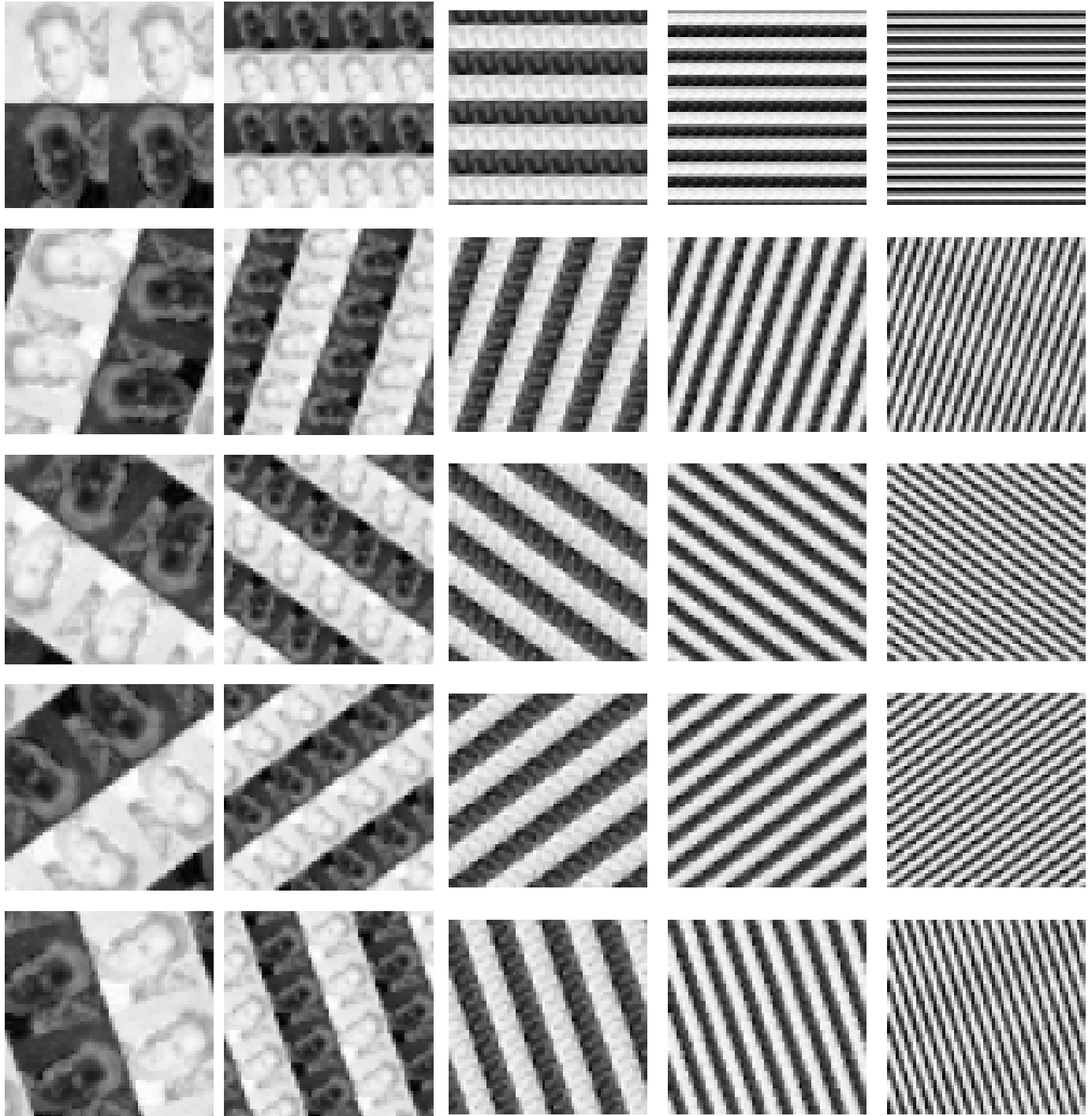


Figure 9.

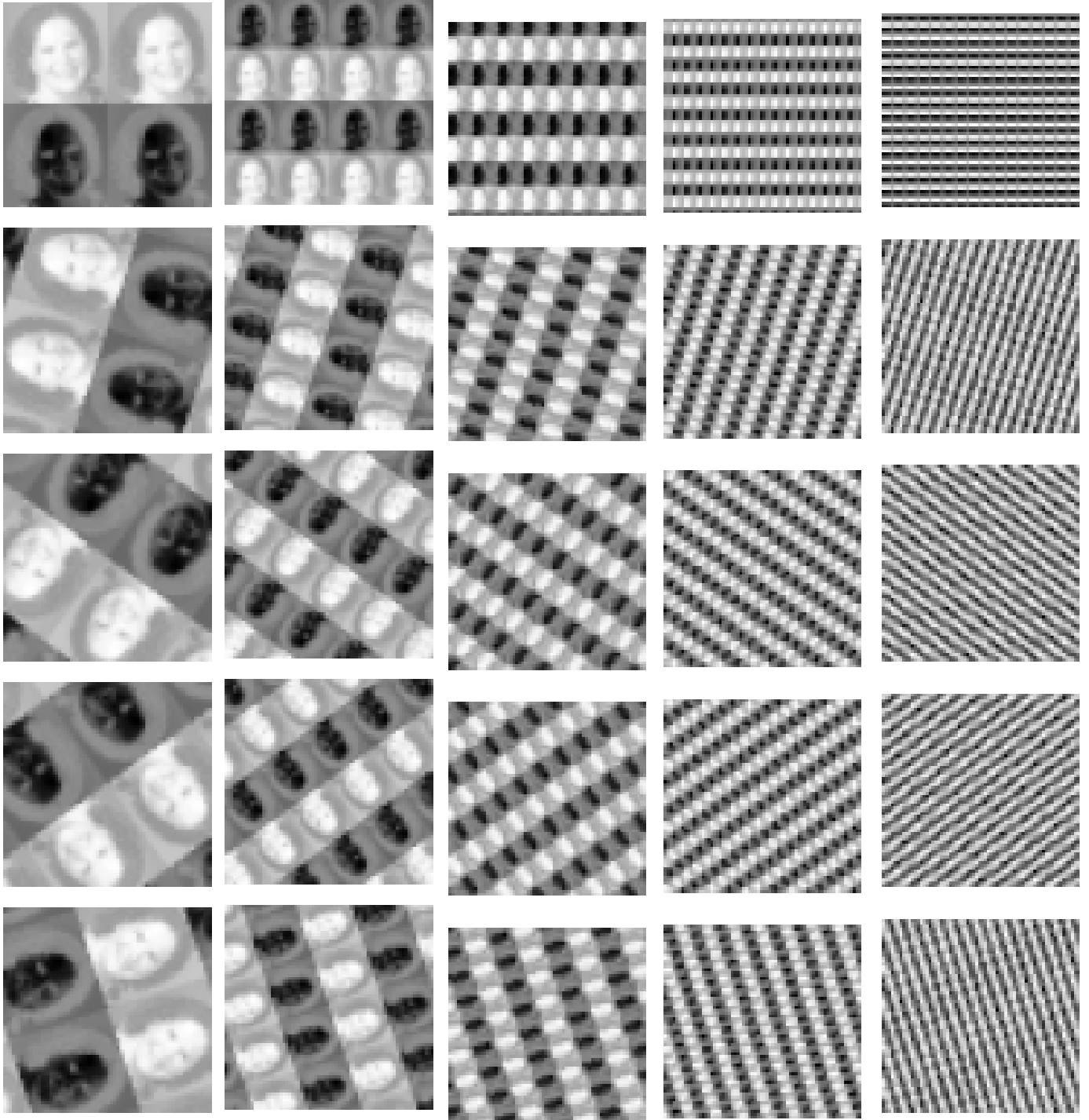
B.6. *Kirkpatrick Basis*

Figure 10.

B.7. *Macintosh Basis*

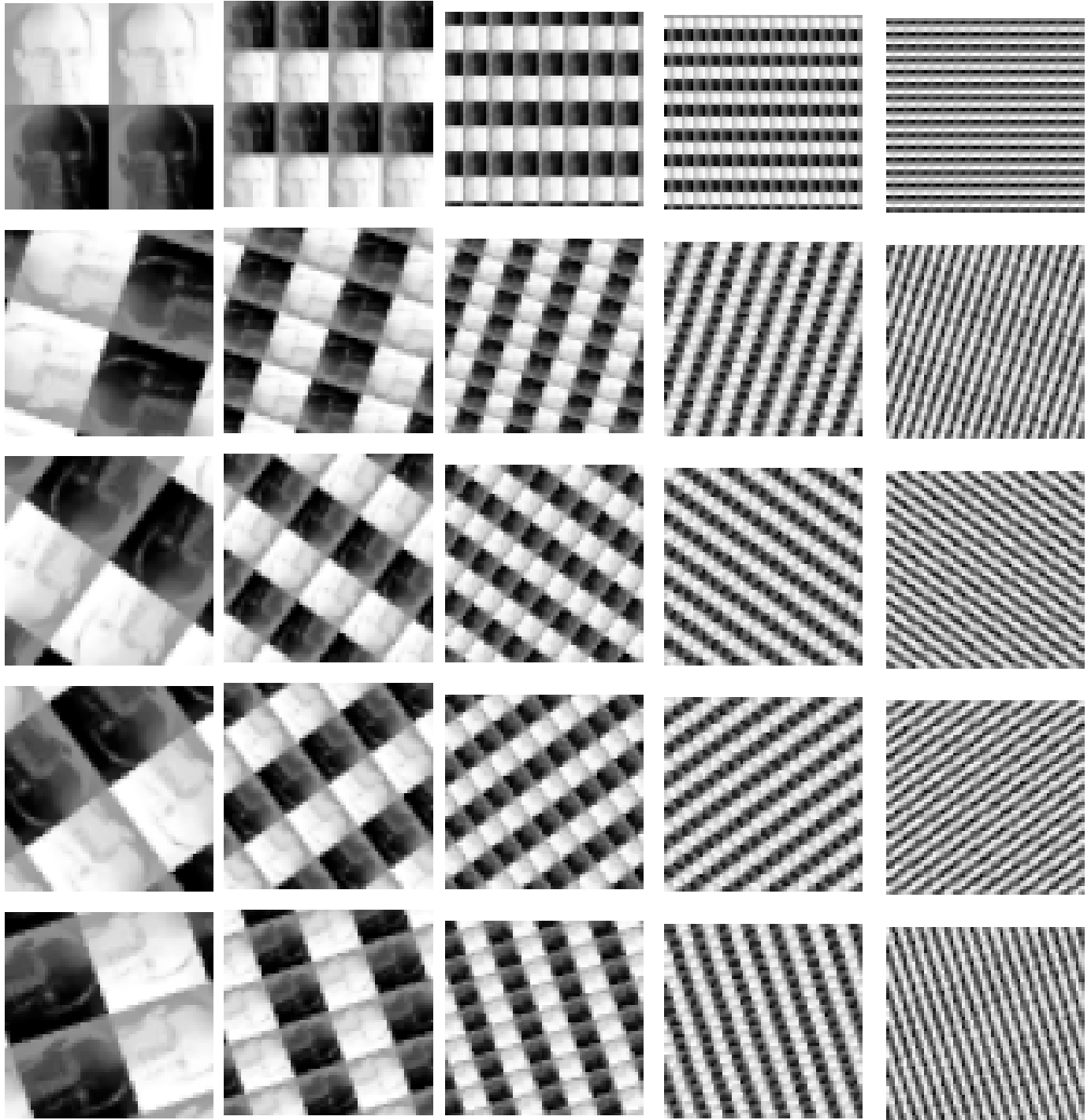


Figure 11.

B.8. *Pearce Basis*

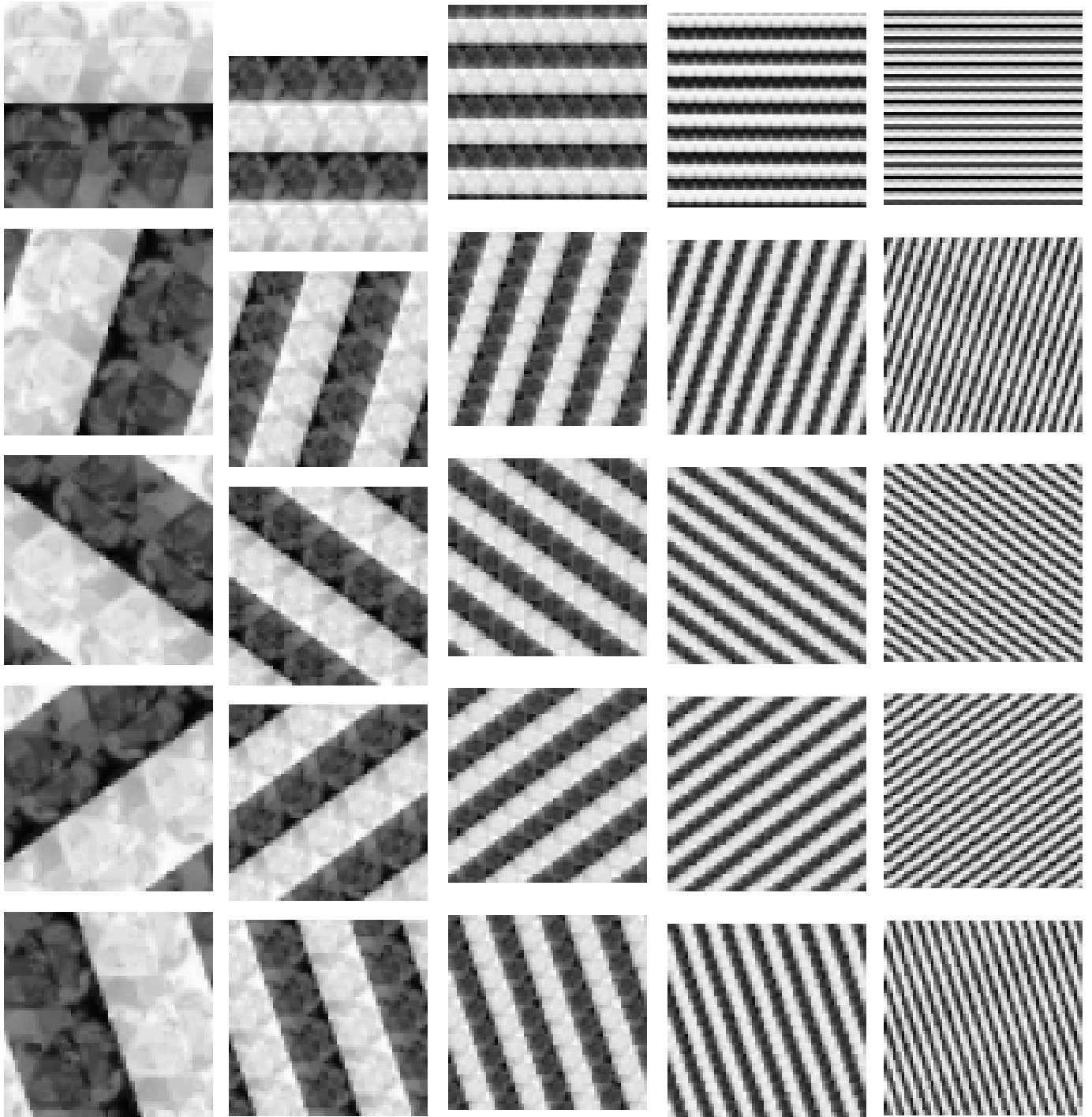


Figure 12.

B.9. *Stelter Basis*

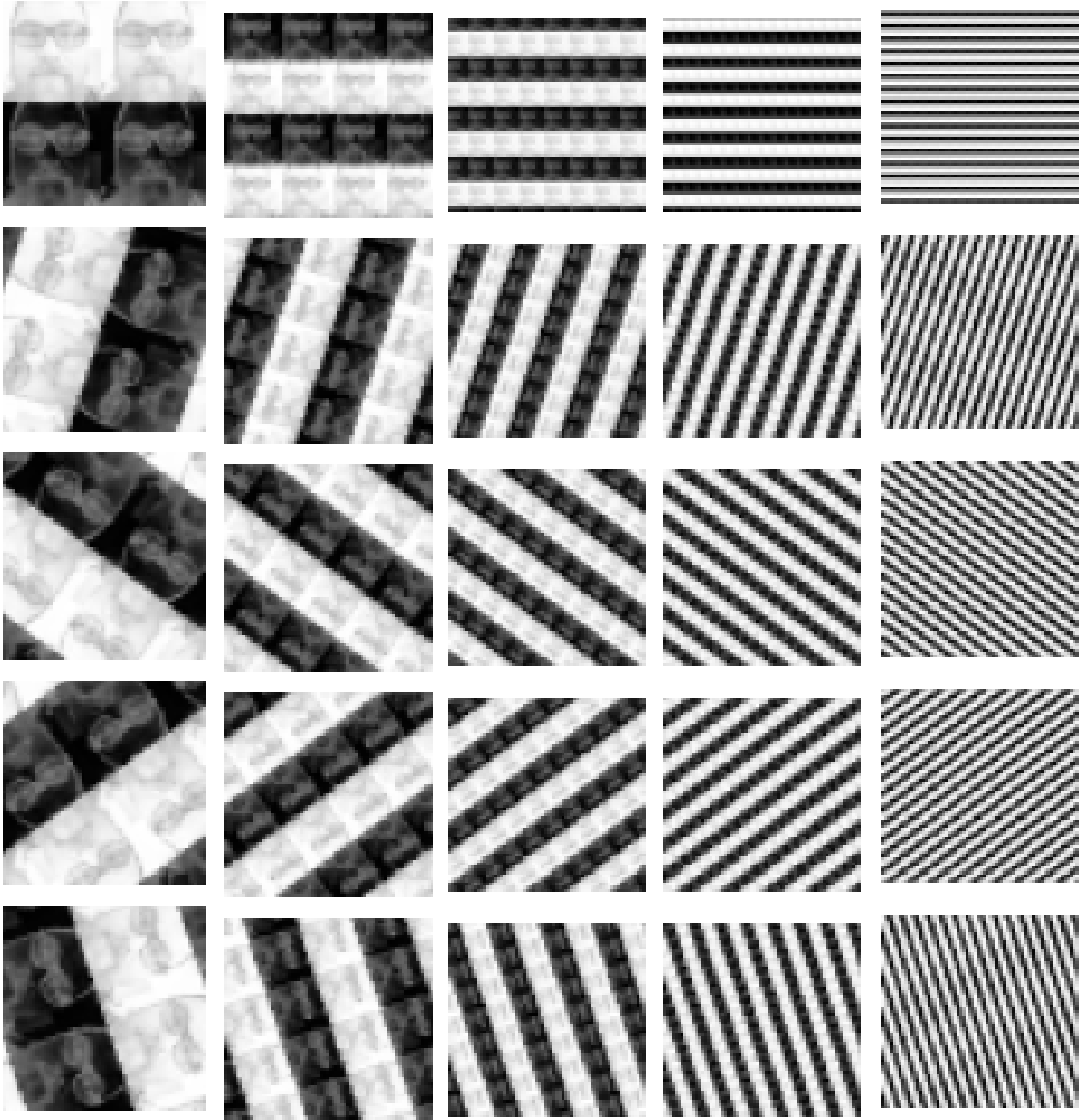


Figure 13.

B.10. *Jensen-Clem Basis*

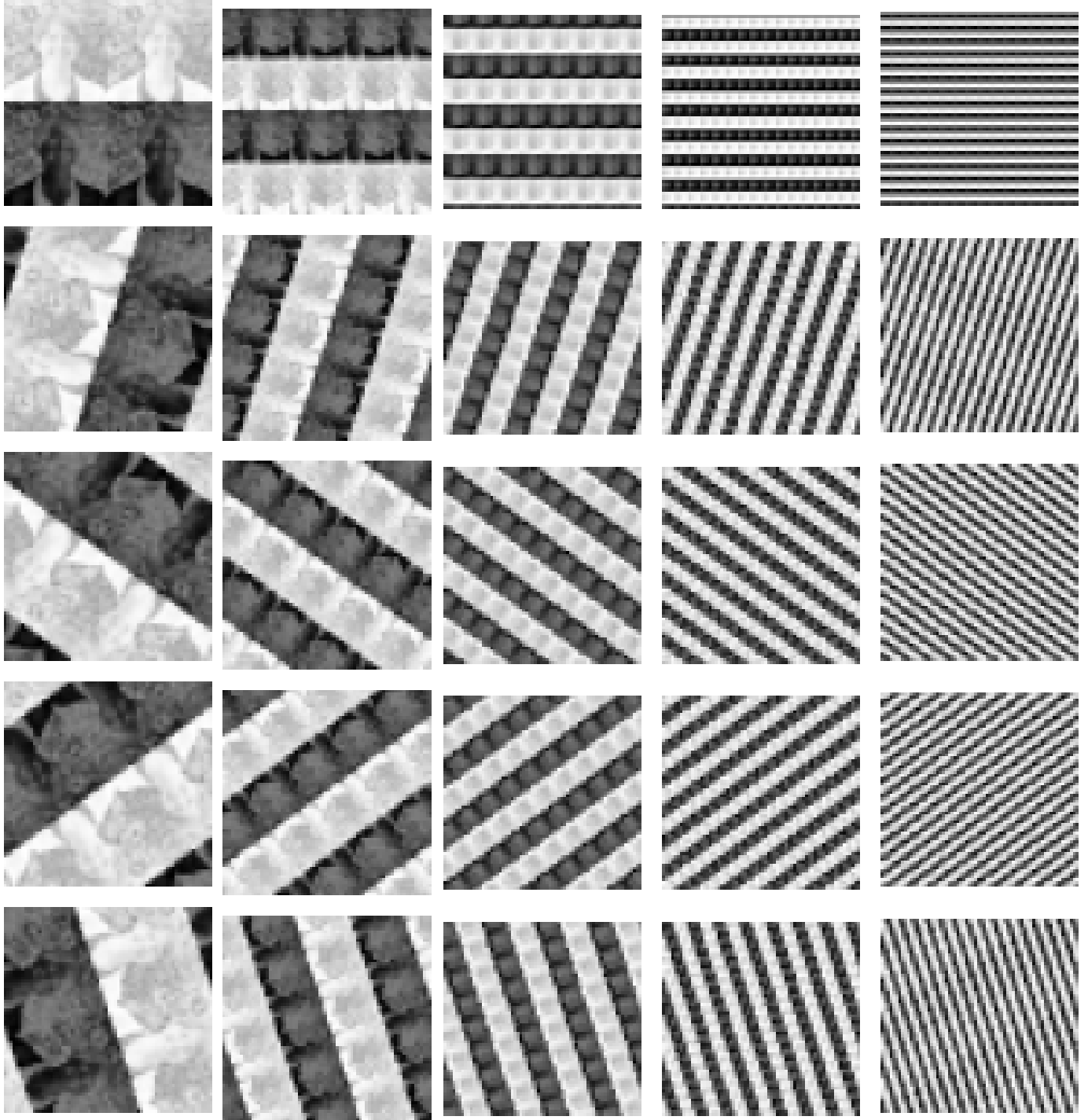


Figure 14.

B.11. *Ngo Basis*

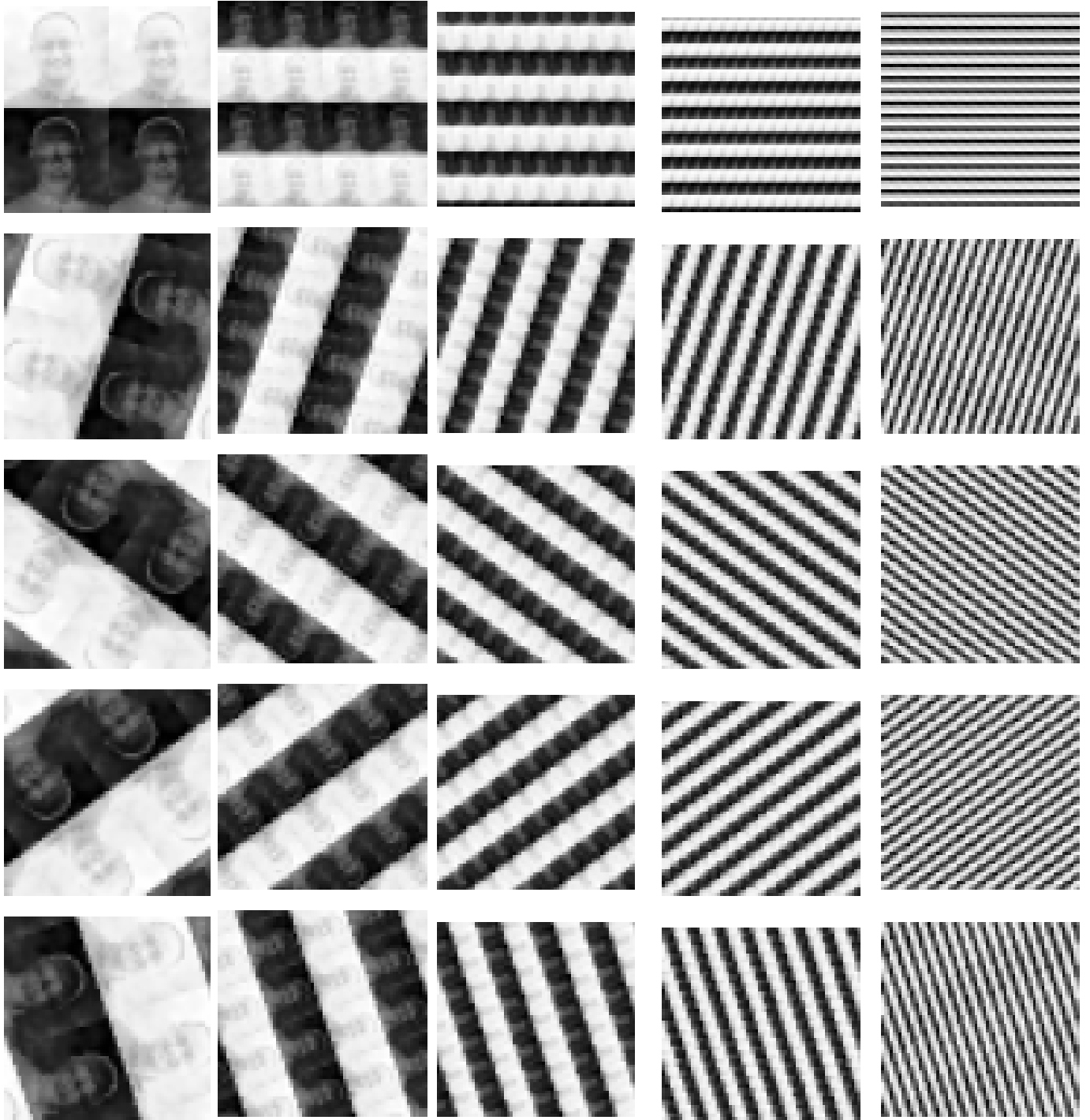


Figure 15.

B.12. *Bowens-Rubin Basis*

123

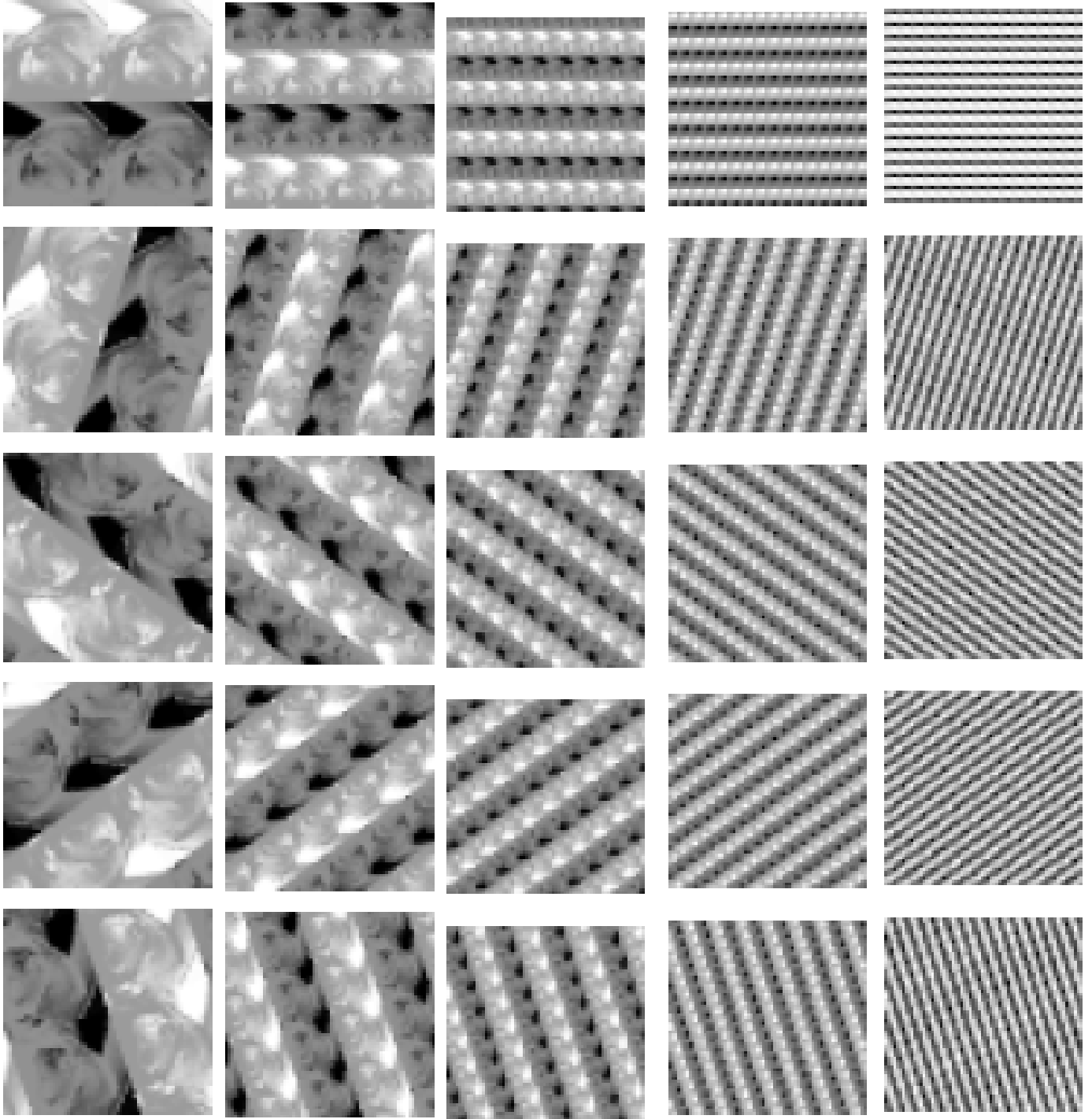


Figure 16.

B.13. *Steiger Basis*

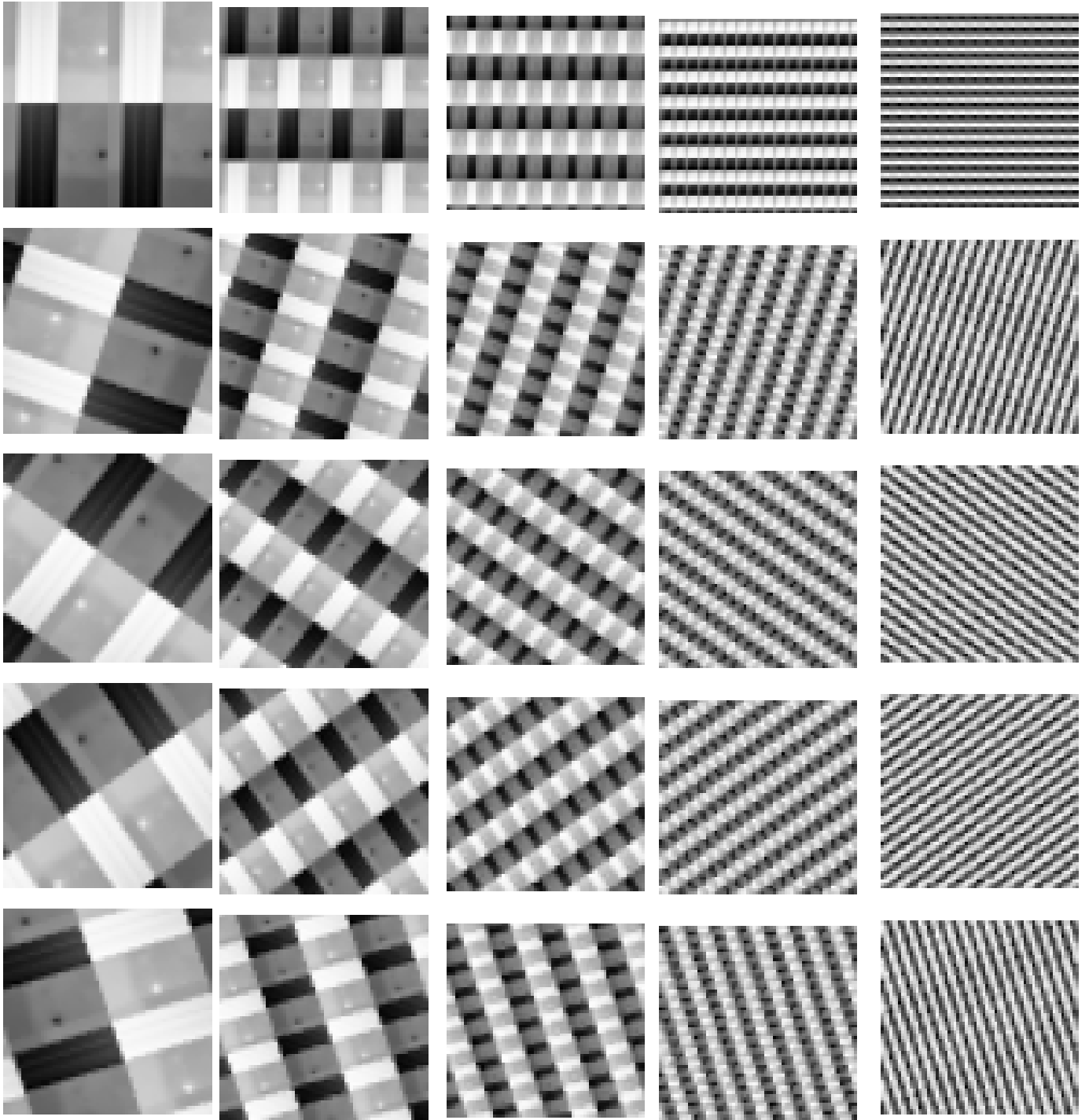


Figure 17.

B.14. *Lewis Basis*

125

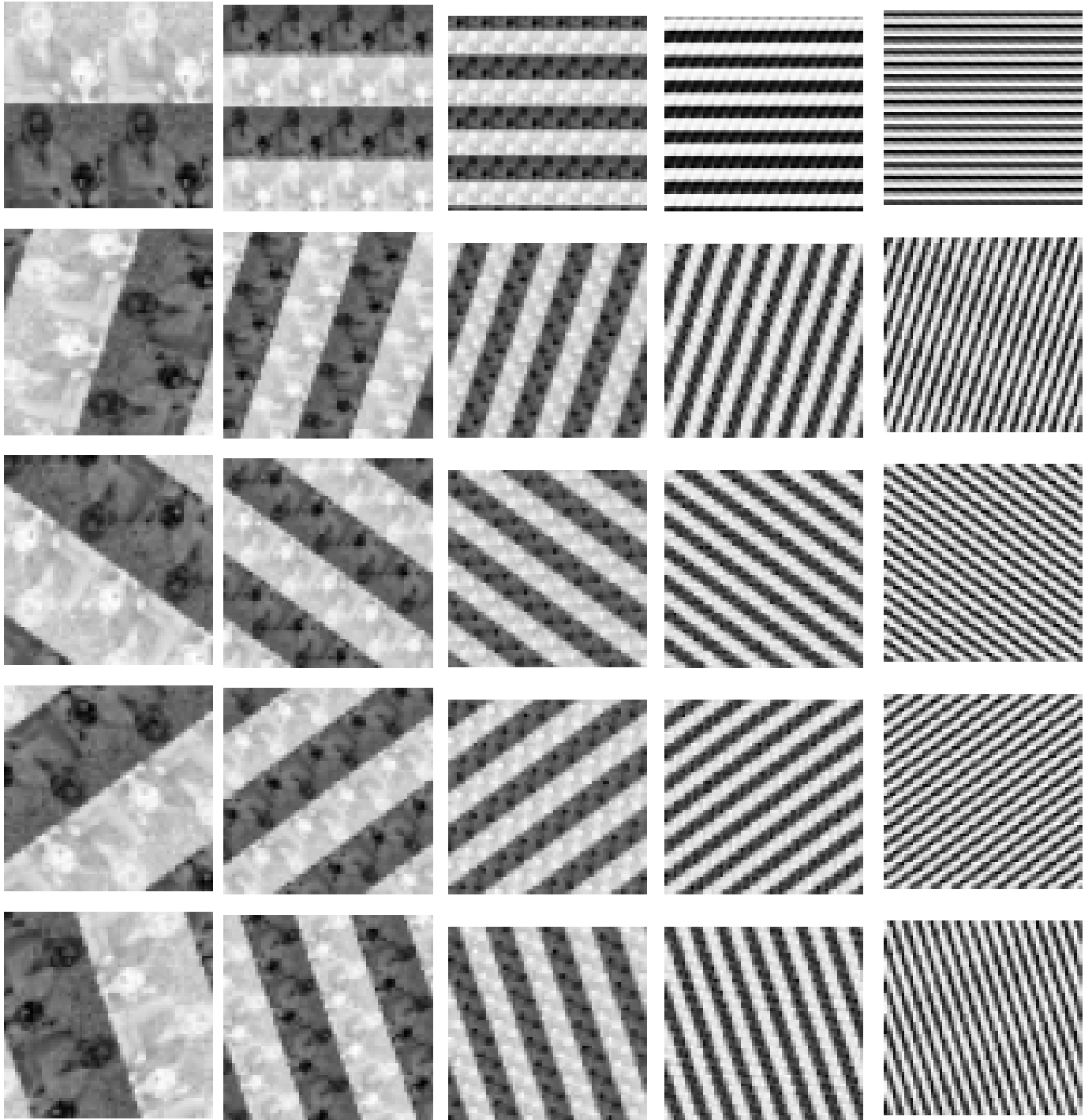


Figure 18.

B.15. *Balmer Basis*

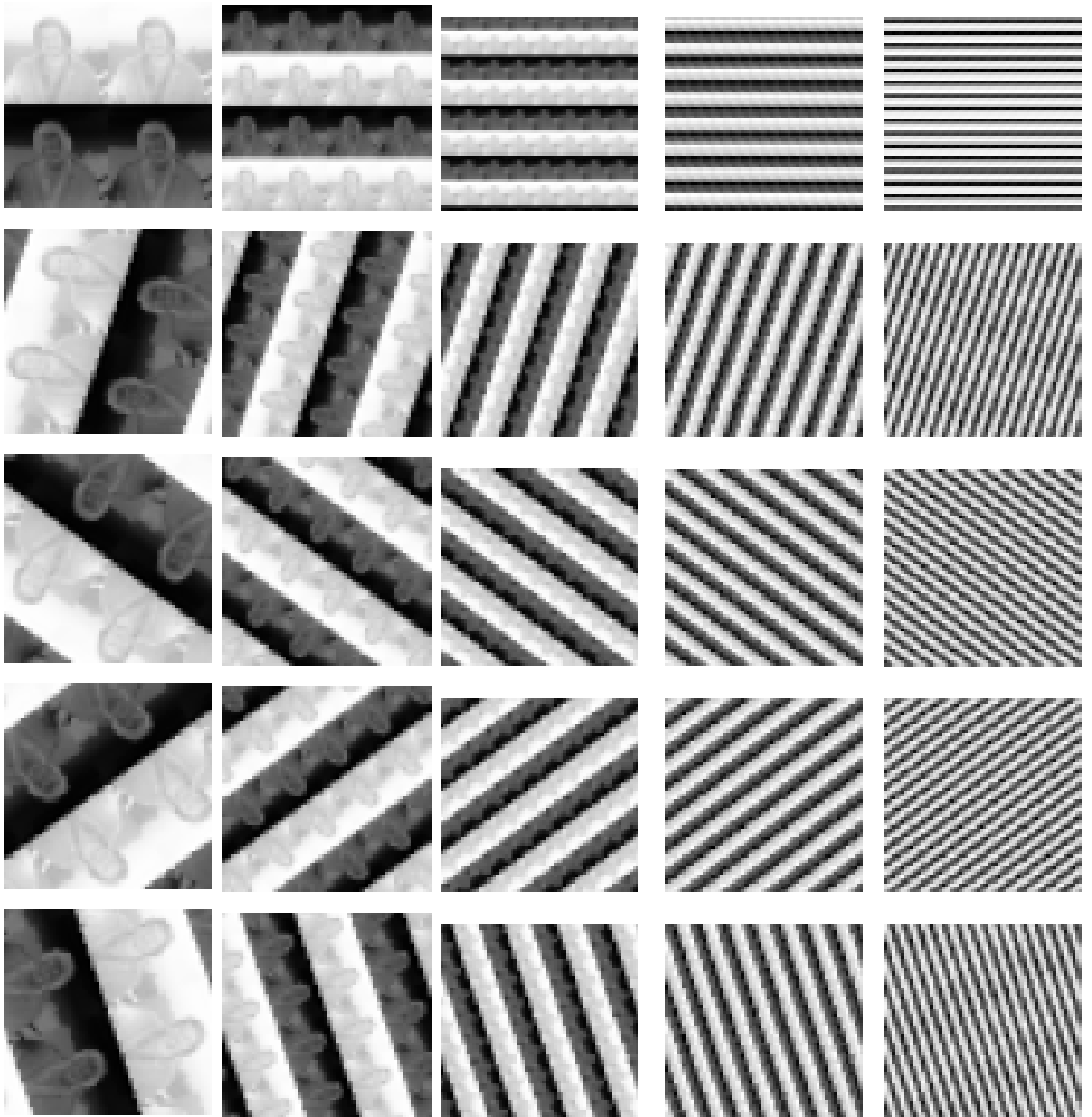


Figure 19.

REFERENCES

- 127 Astropy Collaboration, Price-Whelan, A. M., Sipőcz, B. M.,
128 et al. 2018, *AJ*, 156, 123, doi: [10.3847/1538-3881/aabc4f](https://doi.org/10.3847/1538-3881/aabc4f)
- 129 Fauvarque, O., Neichel, B., Fusco, T., Sauvage, J.-F., &
130 Girault, O. 2016, *Optica*, 3, 1440,
131 doi: [10.1364/OPTICA.3.001440](https://doi.org/10.1364/OPTICA.3.001440)
- 132 Ferland, G. J., Porter, R. L., van Hoof, P. A. M., et al.
133 2013, *RMxAA*, 49, 137. <https://arxiv.org/abs/1302.4485>
- 134 Green, J. 2019, *Turtles All The Way Down* (Penguin Books)
- 135 Hunter, J. D. 2007, *Computing in Science & Engineering*, 9,
136 90, doi: [10.1109/MCSE.2007.55](https://doi.org/10.1109/MCSE.2007.55)
- 137 Lund, M. B. 2017, doi: [10.48550/ARXIV.1703.10432](https://doi.org/10.48550/ARXIV.1703.10432)
- 138 Lund, M. B., Siverd, R. J., & Stibbons, P. 2018,
139 doi: [10.48550/ARXIV.1804.00419](https://doi.org/10.48550/ARXIV.1804.00419)
- 140 Mayorga, L. C., May, E. M., Lustig-Yaeger, J., & Moran,
141 S. E. 2021. <https://arxiv.org/abs/2103.16636>
- 142 Por, E. H., Haffert, S. Y., Radhakrishnan, V. M., et al.
143 2018, in *Proc. SPIE*, Vol. 10703, Adaptive Optics
144 Systems VI, doi: [10.1117/12.2314407](https://doi.org/10.1117/12.2314407)
- 145 Poyneer, L. A., Macintosh, B. A., & Véran, J.-P. 2007,
146 *Journal of the Optical Society of America A*, 24, 2645,
147 doi: [10.1364/JOSAA.24.002645](https://doi.org/10.1364/JOSAA.24.002645)
- 148 Shatokhina, I., Hutterer, V., & Ramlau, R. 2020, *Journal of*
149 *Astronomical Telescopes, Instruments, and Systems*, 6,
150 010901, doi: [10.1117/1.JATIS.6.1.010901](https://doi.org/10.1117/1.JATIS.6.1.010901)
- 151 Stangalini, M., Moro, D. D., Berrilli, F., & von der Lüche,
152 O. 2010, *ApOpt*, 49, 2090, doi: [10.1364/AO.49.002090](https://doi.org/10.1364/AO.49.002090)
- 153 Umesh, P. 2012, *CSI Communications*, 23